Determination of diapycnal diffusion rates in the upper thermocline in the North Atlantic Ocean using sulfur hexafluoride

Dae-Oak Kim, Kitack Lee, and Sung-Deuk Choi

School of Environmental Science and Engineering, Pohang University of Science and Technology, Pohang, Korea

Hee-Sook Kang[1] and Jia-Zhong Zhang

Atlantic Oceanographic and Meteorological Laboratory/NOAA, Miami, Florida, USA

Yoon-Seok Chang

School of Environmental Science and Engineering, Pohang University of Science and Technology, Pohang, Korea

[1]   The apparent diapycnal diffusivity below the wind-driven surface mixed layer of the ocean was determined in an anticyclonic eddy in the eastern North Atlantic using sulfur hexafluoride (SF_6) tracer data collected in June 1998. In this tracer experiment the downward penetration of SF_6 was measured for 3 weeks following the deliberate injection of SF_6 in the surface mixed layer. The resulting data were used to constrain the one-dimensional Fickian diffusion model to estimate the diapycnal diffusivity. The model also includes the lateral diffusion component so that it can more accurately represent the time evolution of the SF_6 concentrations along the isopycnal surface. This affects the estimation of the diapycnal diffusivity. For the upper thermocline immediately below the surface mixed layer we estimated the diapycnal diffusivity for the 3 week period as 0.3 ± 0.2 cm^2 s^{-1} at a buoyancy frequency of 8.2 cph.

Citation: Kim, D.-O., K. Lee, S.-D. Choi, H.-S. Kang, J.-Z. Zhang, and Y.-S. Chang (2005), Determination of diapycnal diffusion rates in the upper thermocline in the North Atlantic Ocean using sulfur hexafluoride, *J. Geophys. Res.*, *110*, C10010, doi:10.1029/2004JC002835.

1.   Introduction

[2]   In oceans, heat, salts, and nutrients are redistributed more rapidly within water masses of uniform density than across surfaces separating waters of different densities. Nonetheless, accurate representation of diapycnal eddy diffusion in oceans is an important requirement for numerical models of climate change, biological productivity, and the viability of deep sea disposal of carbon and radioactive waste [*Munk*, 1966; *Bryan*, 1987; *Gargett*, 1993]. For most of the upper oceans, the surface biological productivity is generally limited by nitrate availability [*Eppley and Peterson*, 1979]. The flux of nitrate from nitrate-replete deep water to the impoverished upper ocean dominates the supply of nitrogen for the 75% of the world's ocean that is considered oligotrophic [*Lewis et al.*, 1986]. However, estimation of this vertical flux of nitrate has proved difficult due to limited knowledge of the mechanisms and factors affecting nitrate transport across density surfaces.

[3]   The rate at which the seawater within the pycnocline is vertically mixing can be directly estimated from measurements of the vertical spreading of a deliberately released substance over time, assuming that the released tracer and seawater move together. In this case, estimated diapycnal eddy diffusivity (K_V) accounts for the contributions of all of the mixing processes to the observed distribution of the tracer integrated over the timescale of the measurements, and it is referred to as "apparent" or "effective" eddy diffusivity. Fluorescent dyes have been extensively used to measure the K_V in the stratified ocean. However, dye experiments suffer from several drawbacks. The duration of such experiments is limited to a few days because of relatively low sensitivity and progressive dye degradation [*Woods*, 1968; *Schuert*, 1970; *Ewart and Bendiner*, 1981; *Vasholz and Crawford*, 1985]. Dyes are toxic and expensive. The introduction of sulfur hexafluoride (SF_6) as a deliberate tracer has overcome these limitations and made longer experiments possible. SF_6 is superior to dyes for use in measuring diapycnal diffusivity in the open ocean for a variety of reasons, including its low background concentration in the marine environment (<2 fM, fM = 10^{-15} mol L^{-1}), its low detection limit (<1 fM, which is $\sim 10^6$ times lower than the detection limit for fluorescent dyes), and its nontoxicity and inertness. The maximum duration of surface SF_6 tracer experiments are largely determined by the rate of SF_6 loss to the atmosphere due to gas exchange.

[4]   Because SF_6 is a conservative tracer after isolation from the surface mixed layer, measurements of its penetration into the upper thermocline can be used to estimate K_V. Studies using SF_6 integrate over a range of mixing scales,

thus producing bulk estimates of diapycnal mixing that can be useful in ocean circulation models. Several SF_6 Lagrangian tracer experiments have been conducted in or just below the surface mixed layer [*Watson et al.*, 1991; *Wanninkhof et al.*, 1997; *Law et al.*, 1998, 2001, 2003]. Results from three of these experiments have been used to estimate K_V [*Law et al.*, 1998, 2001, 2003]. More measurements under different environmental forcing conditions are necessary to resolve how physical factors affect the rate of diapycnal diffusion. In this paper, we estimate K_V immediately below the surface mixed layer using the 1-D Fickian diffusion model constrained with the 3 week evolution of the vertical penetration of SF_6 in an anticyclonic eddy in the eastern North Atlantic. This study differs from those carried out previously in that our tracer experiment covered a longer period of time.

2. Field SF_6 Data Used to Estimate K_V

2.1. Release of SF_6

[5] An anticyclonic eddy located at about 46°N and 20.5°W in the eastern North Atlantic was chosen as a study site [*McGillis et al.*, 2001]. A mixture of SF_6 (99.7% v/v) and ^{3}He (0.3% v/v) was released at a depth of 12–15 m over a 7 km band by bubbling the gases into the water column through a 0.5 m porous tube. A total of 20 mol of SF_6 and 0.06 mol of ^{3}He were released at the base of the surface mixed layer. The gas transfer velocity was determined by measuring differences in escaping velocity of SF_6 and ^{3}He and by micro meteorological techniques [*McGillis et al.*, 2001]. Three ARGOS, one GPS, and two CARIOCA buoys [*Merlivat and Brault*, 1995] were concurrently deployed to follow the movement of the SF_6 patch. Most of the survey, which was carried out during the 3 weeks following gas injection, was performed inside of the eddy (Figure 1). Comparison of ARGOS buoy positions with the SF_6 patch and the altimetry data suggested that the SF_6 patch remained within the eddy for the duration of this experiment.

2.2. Chemical Analysis for Released SF_6

[6] An automated discrete system, modeled after that used by *Upstill-Goddard et al.* [1991], was used to determine the SF_6 content in seawater samples that were collected each day from two to three CTD casts within the tracer patch. The discrete system consists of a gas chromatograph (GC) equipped with an electron capture detector, a SF_6 stripping chamber, a SF_6-trapping device, and an integrator. For samples taken during the first week of the experiment, which contained high [SF_6] (great than ~1 × 10^{-13} M), syringes were filled to 30 mL with seawater from the Niskin bottles, and a headspace was created by adding 20 mL of N_2. Syringes were then mechanically shaken for 10 min to equilibrate the samples with N_2. The equilibrated headspace gas was injected into the GC. For samples taken during the last 2 weeks of the experiment, which were characterized by low [SF_6] (less than ~1 × 10^{-13} M), samples were taken in 500 mL bottles. About 225 mL of sample was introduced into a stripping chamber by vacuum. A continuous flow of N_2 stripped the SF_6 from the seawater aliquot, and this SF_6 was trapped on a CARBOXEN 1000 (60/80 mesh)-filled stainless steel trap immersed in isopropanol chilled to
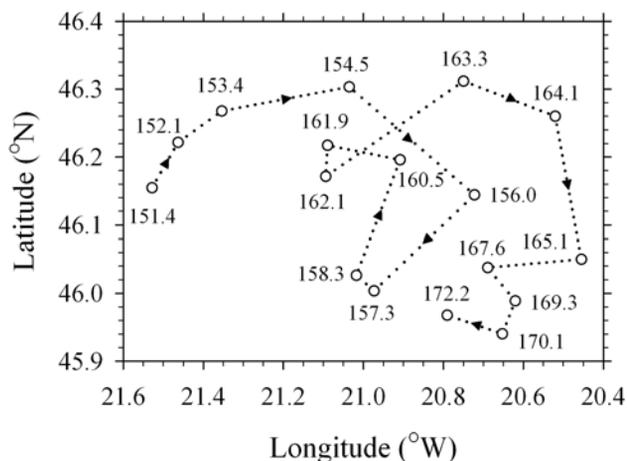

Figure 1. Locations of the daily maximum SF_6 concentration in the surface mixed layer during the GasEx-98 cruise.

−60°C. SF_6 was then released by heating the trap to 160°C. Comparison of the standard gases transferred directly from the sample loop to the GC column with the same standards transferred from the sample loop to the trap and then to the column showed that the trapping efficiency was nearly 100%. The absence of a SF_6 peak after the second stripping of samples with N_2 verified that the stripping efficiency was also 100%. Finally, the reproducibility of the discrete system was better than 0.5%.

[7] The surface [SF_6] was continuously mapped by an automated underway system that samples water pumped at 5 L min^{-1} from the bow at a depth of 6 m. The underway system consists of a GC equipped with an electron capture detector, a SF_6 stripping device (Liqui-Cel® membrane contactor), and an integrator. The membrane contactor extracts SF_6 from seawater through hollow gas permeable membrane fibers into N_2 carrier gas, which sweeps the SF_6 into a GC for analysis. The underway data were corrected for the efficiency of the stripping device, which was monitored throughout the cruise by comparing underway and batch SF_6 measurements from the same samples.

3. Results and Discussions

3.1. Environmental Conditions Within the Eddy

[8] The anticyclonic eddy chosen as the study site largely maintained a discrete body of water with physical and biogeochemical characteristics different from those of the surrounding water. During the experiment, six atmospheric disturbances passed through the study site with wind speeds greater than 8 m s^{-1}, each of which lasted 2–4 days (Figure 2a). These storm events were strongly correlated with decreases in atmospheric pressure. Wind speeds of up to 18 m s^{-1} were recorded during the largest storm event, which occurred between 6 and 10 June (YD 158–162). The storm events increased the mixed layer depth, suggesting that the timing of mixed layer deepening and shoaling was probably correlated with variations in the wind speed (Figure 2b). The evolution of seawater density in the surface mixed layer and in the upper thermocline within the patch was mostly a result of the seawater temperature change
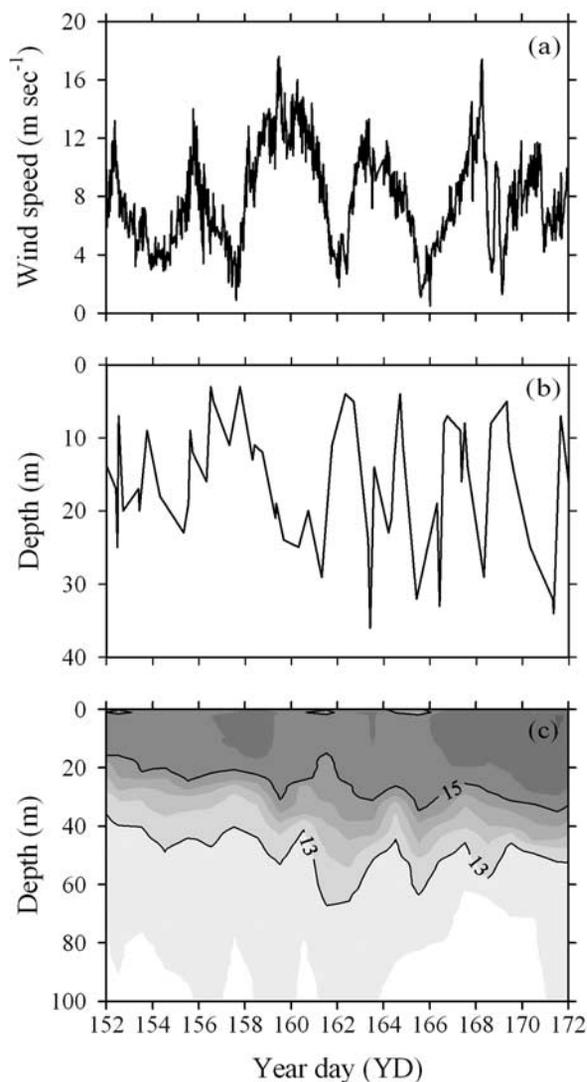
Figure 2. Time records of (a) wind speed, (b) mixed layer depth, and (c) CTD-measured temperature profile for the period of the GasEx-98 cruise.

because salinity within the eddy remained essentially unchanged throughout the experiment. A warming trend was observed in the surface mixed layer and in waters of depth 20–60 m, within which the penetration of SF_6 was confined over the 3 week period (Figure 2c). The evolution of the physical properties of the surface mixed layer and the upper thermocline was essentially controlled by local variations in wind stress and net heat fluxes. This is because the study site was inside an anticyclonic eddy and, therefore, had only limited exchange with contrasting surrounding waters. Surface mixed layers are defined here as the depth where the density gradient with depth ($\partial\rho/\partial Z$) is 0.004 kg m^{-3} m^{-1} [*Price et al.*, 1986].

3.2. Background [SF₆] at the Study Site

[9] SF_6 is commonly used in gas-insulated components of electrical transmission and distribution systems. Most of the SF_6 in these components escapes to the atmosphere within a few decades, where it has a lifetime of about 3200 years. In 1998, the global mean abundance of SF_6 in the atmosphere

was 4.3 parts per trillion by volume (pptv), and it has increased at a rate of ~7% per year (available at http://www.cmdl.noaa.gov). Because of air-sea gas exchange, the presence of SF_6 in the atmosphere results in a background concentration in the upper water column. In the present work, two [SF_6] profiles that were obtained within the eddy prior to SF_6 release were used to determine the background SF_6 concentration. Both profiles showed a constant background [SF_6] of 0.75 ± 0.16 (1σ) fM down to a depth of 200 m. This background SF_6 concentration was subtracted from all subsequent SF_6 measurements and did not significantly affect our experimental results. The background [SF_6] data suggest that the mixed layer was nearly equilibrated with an air mass of mixing ratio 4.3 pptv in 1998, which would yield a background of ~0.9 fM at a seawater temperature of 15°C.

3.3. Continuous Measurements of Surface [SF₆] at the Study Site

[10] After the release of SF_6 into the surface mixed layer, various processes affect the concentration of SF_6 in the surface mixed layer. These processes include lateral diffusion, air-sea gas exchange, entrainment of water from the upper thermocline, and vertical diffusion across the bottom of the surface mixed layer [*Watson et al.*, 1991; *Wanninkhof et al.*, 1997; *Law et al.*, 1998, 2001, 2003; *Park et al.*, 2005], with the former two processes having a much greater effect than the latter two. The loss of SF_6 to the atmosphere ($L_{AIR-SEA}$) was calculated from the measured differences in SF_6 concentrations between seawater (SF_{6-SW}) and air (SF_{6-AIR}) and an empirical gas transfer velocity (k): $L_{AIR-SEA} = k$ ($SF_{6-SW} - SF_{6-AIR}$). During the present tracer experiment, the term $SF_{6-SW} - SF_{6-AIR}$ was nearly equal to SF_{6-SW} because SF_6 concentrations in seawater were several orders of magnitude greater than those in air. In this calculation, we obtained k using the following empirical relationship [*Wanninkhof and McGillis*, 1999] derived using results from a covariance flux study during the GasEx-98 cruise [*McGillis et al.*, 2001]: $k = 0.0283 \ WS_{10}^3 \ (Sc/660)^{-1/2}$, where Sc is the Schmidt number for SF_6 and WS_{10} is the wind speed in m s^{-1} at a height of 10 m. This cubic relationship predicts that gas transfer is weaker at low wind speed and stronger at high wind speed.

[11] Changes in the mixed layer SF_6 concentration due to horizontal diffusion were estimated from differences between the measured [SF_6] and the [SF_6] predicted for the case in which the only factor affecting [SF_6] is loss of SF_6 to the atmosphere (the dashed line in Figure 3a). Figure 3b shows the relative contributions of lateral diffusion and gas exchange processes to the decrease in the mixed layer [SF_6]. The lateral diffusion-induced decrease in [SF_6] accounts for the majority of the total loss of SF_6 for the period YD152−156, whereas loss to the atmosphere due to gas exchange becomes important during the last 2 weeks of the experiment (YD157−172).

[12] The rate of decrease in surface [SF_6] for the period YD 151−160 is significantly higher than that for the period YD 161−172. The exact cause for the discontinuity in the exponential decay of surface [SF_6] at day 160 has yet to be identified. One possible explanation is that, over the 10 day period (YD 151−160) following SF_6 injection, the SF_6 patch grew to a substantial size through lateral diffusion
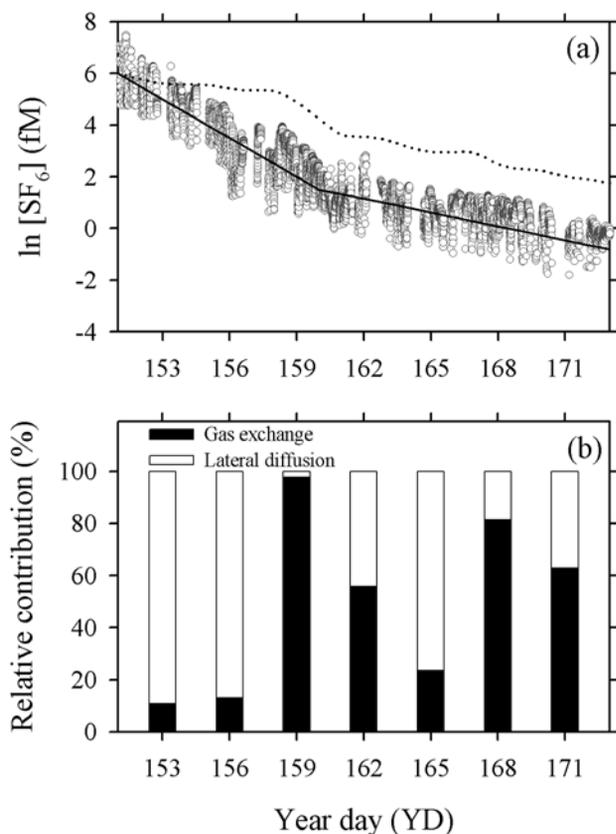
Figure 3. (a) Underway measurements of surface SF_6 concentration ($[SF_6]$, fM) over the 3 week period. Two equations of $\ln [SF_6] = 81.5 - 0.5$ YD and $\ln [SF_6] = 30.07 - 0.1785$ YD were generated to represent the periods of YD = $151-160$ and YD = $161-172$, respectively. The solid line is the best fit of the data. The expected decline of surface $[SF_6]$ based on loss to the atmosphere (dashed line) was estimated using a parameterization of *Wanninkhof and McGillis* [1999] and daily mean surface mixed layer depths. (b) Percent (%) loss of SF_6 at the patch center due to gas exchange (filled bars) and lateral diffusion (open bars). Results are grouped into 3 day intervals.

of SF_6 in all directions within the eddy. As a result, the SF_6 concentration within the tracer patch rapidly decreased during this period. At YD 160, part of the SF_6 patch appeared to reach the boundary between the eddy and the surrounding water with contrasting physical properties (data not shown). This impingement of the patch on the boundary likely hindered the transport of SF_6 by lateral diffusion, causing a lower rate of decrease in the mixed layer $[SF_6]$ relative to the rate observed for the period prior to YD 160. However, this hypothesis cannot be tested using the available data.

3.4. Vertical Distribution of $[SF_6]$ in the Upper Thermocline

[13] The daily vertical profiling of $[SF_6]$ was undertaken near the center of the patch to minimize the impact of lateral mixing between the SF_6 patch and the SF_6-free surrounding water. Figure 4 shows the evolution of the measured $[SF_6]$ profile within the patch; the data in this figure were obtained using at least two profiles per day. We used all $[SF_6]$ profiles

($n = 60$) that had surface concentrations greater than 10% of the daily maximum, as determined from the underway measurements. In each $[SF_6]$ profile, two times the background concentration (~ 1.5 fM) was used as a cutoff.

[14] The SF_6 that was initially injected into the surface mixed layer penetrated to a depth of ~ 40 m during the first 10 days and then gradually migrated down to ~ 60 m through the upper thermocline (Figure 4). Several storms transported SF_6 vertically by advection through deepening of the surface mixed layer. However, it is not clear from the available SF_6 data whether the storm events enhanced SF_6 transport by diapycnal diffusion.

3.5. Estimation of K_V

[15] In the estimation of K_V using SF_6 data, we assumed that the diapycnal diffusion was exclusively responsible for vertical SF_6 penetration within the depth range of $20-60$ m in the upper thermocline (Figure 5). Because the vertical sampling of the SF_6 distribution was not sufficiently resolved to determine the depth dependence of K_V, we additionally assumed that K_V was constant over the same depth range, within which $[SF_6]$ rapidly decreased. To estimate K_V in the upper thermocline, the 1-D Fickian diffusion model was constrained with the 3 week evolution of SF_6 down through the upper thermocline. In this 1-D diffusion model, the downward flux of SF_6 (F_Z, mol m^{-2} s^{-1}) into the upper thermocline was estimated from the vertical gradient of SF_6 concentration ($d[SF_6]/dZ$) immediately below the mixed layer multiplied by diapycnal eddy diffusivity (K_V, m^2 s^{-1}):

$$F_Z = -K_V(d[SF_6]/dZ), \qquad (1)$$

where Z (m) is taken positive downward with $Z = 0$ at the surface.

[16] Simulations using the 1-D diffusion model were performed using the same resolution of hydrocast sampling; approximately twice per day near the center of the SF_6 patch. The model simulations were initialized using data from YD 151.6 (31 May 1998) with the water column profile of $[SF_6]$. The simulations were then integrated forward in time to YD 172 (24 June 1998). At each time
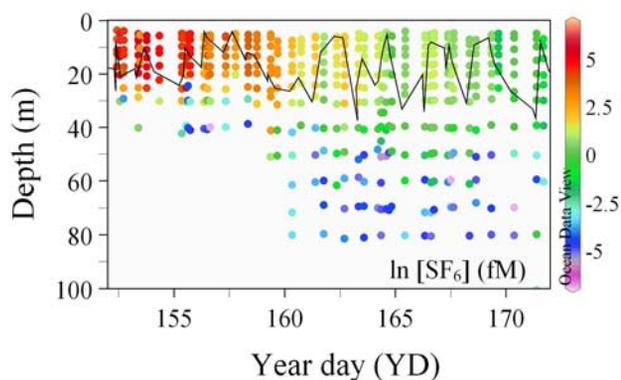

Figure 4. Vertical distribution of SF_6 concentration ($\ln [SF_6]$, fM) at the patch center during the GasEx-98 cruise. The solid line represents mixed layer depths (m).
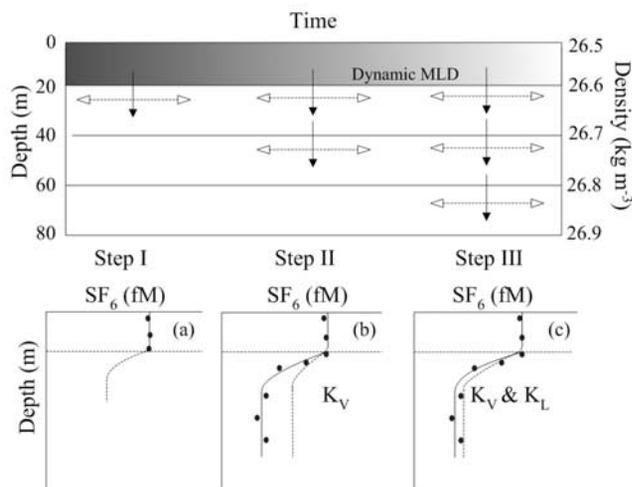
Figure 5. A schematic of the one-dimensional Fickian diffusion model showing the sequence of the model simulations for estimating K_V: (a) constraining the 1-D model with the [SF$_6$] profile modeled at the previous time step, (b) vertical penetration of SF$_6$ by diapycnal diffusion (K_V), and (c) lateral diffusion of SF$_6$ along the isopycnal surface using a measured rate (K_L) of [SF$_6$] decrease in a depth range of 20–60 m. The shading in the uppermost layer indicates changes in SF$_6$ concentration in the dynamic mixed layer (MLD) during the duration of the experiment. The solid and dashed lines in Figures 5a–5c represent the best fits of measured and modeled [SF$_6$] profiles, respectively.

step, the model was first forced to the new mixed layer [SF$_6$] (the solid line in Figure 5a) estimated from one of two linear equations (see the caption of Figure 3a) derived from continuous measurements of surface [SF$_6$]. This procedure provided a reliable source function of the mixed layer [SF$_6$] by collectively accounting for decrease in [SF$_6$] due to air-sea exchange and lateral diffusion (see Figure 3b). Second, the diffusive flux of SF$_6$ from the base of the mixed layer to the uppermost thermocline and subsequently down through the thermocline was modeled by the K_V multiplied by the vertical gradient of [SF$_6$] (the dashed line in Figure 5a) modeled at the immediately previous time step. This vertical flux of SF$_6$ produced a new [SF$_6$] profile (the dashed line in Figure 5b).

[17] Since SF$_6$ simultaneously diffuses across density surfaces and along the isopycnal surface in the upper thermocline, in modeling the time evolution of the [SF$_6$] profile, a mean rate of [SF$_6$] decrease by lateral diffusion in conjunction with a K_V was applied uniformly below the bottom of the mixed layer. Only two daily vertical profiling of [SF$_6$] undertaken near the center of the patch was not broad enough to obtain a good estimate of the evolution of [SF$_6$] in the upper thermocline of the entire patch. For each measurement interval, several [SF$_6$] profiles representing the isopycnal distribution of [SF$_6$] in the upper thermocline of the entire patch are needed to obtain the lateral diffusivity. Therefore in modeling the evolution of [SF$_6$] along the isopycnal surface, the mean measured rate of [SF$_6$] decrease rather than a lateral diffusivity coefficient was used. At each time step of the model simulations, the diapycnal diffusion

process transported SF$_6$ down through the upper thermocine, resulting in an increase in [SF$_6$] for each layer in the upper thermocline. The SF$_6$ concentration for each layer was subsequently diluted by the lateral diffusion process (the dashed line Figure 5c). To model lateral diffusive transport of SF$_6$, the mean rate of measured [SF$_6$] decrease in the 20–60 m depth range was used because the rate appeared to be independent of depth for this depth range (equivalent to $\sigma_\theta = 26.3$–26.9) (Figure 6). The incorporation of the lateral diffusion component in the Fickian model reproduced more accurately the time evolution of the [SF$_6$] profile, which in turn affects the estimation of K_V. The value of K_V was chosen to be the value for which the evolution of the modeled [SF$_6$] profile was most consistent with the field observations (Figures 7a and 7b).

[18] To accentuate the vertical penetration of SF$_6$ with time, the SF$_6$ concentrations were normalized by the maximum concentration in each profile, [SF$_{6MAX}$]. The maximum values of [SF$_6$], represented by a contour line of 1.0, were generally found near the bottom of the surface mixed layer (Figure 7a). The key criterion that determined which value of K_V yielded results that were most consistent with the field observations was not the evolution of a particular [SF$_6$]/[SF$_{6MAX}$] isopleth but rather the 3 week evolution of the [SF$_6$]/[SF$_{6MAX}$] profile (Figure 7a); the optimal value of K_V was taken as the value that gave a minimum least squared difference between the measured and predicted [SF$_6$] data (Figure 7c). The 1-D Fickian model constrained with the 3 week evolution of the [SF$_6$]/[SF$_{6MAX}$] profile yielded a K_V of 0.3 cm^2 s^{-1}.

[19] In the modeling of K_V using SF$_6$ data, we did not use two [SF$_6$] profiles obtained at YD 159.4 and 165.4, because a few erroneous [SF$_6$] data in these profiles probably caused local maximums in [SF$_6$]/[SF$_{6MAX}$] at ~40 m. Another
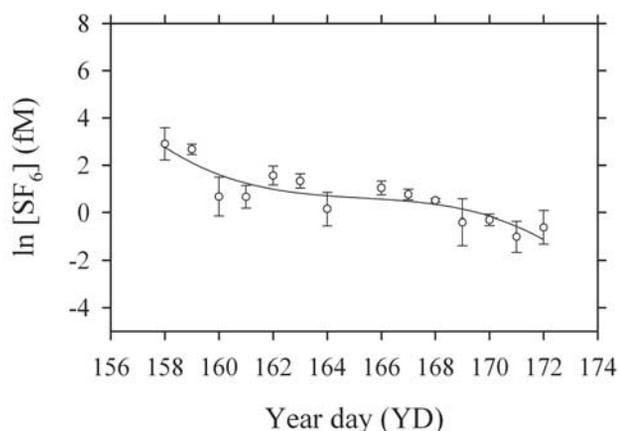

Figure 6. Evolution of measured mean SF$_6$ concentration ([SF$_6$], fM) for waters in a 20–60 m depth range. [SF$_6$] data obtained prior to YD 157 for waters in the upper thermocline are not included in the plot because vertical SF$_6$ penetration was minimal during the first week of the experiment. The measured [SF$_6$] data for waters in the 20–60 m depth range are grouped into 3 day intervals, and a mean value for each 3 day interval is then obtained. Error bars represent standard deviations (1σ) of the differences in each group. The solid line is the best fit of the data.
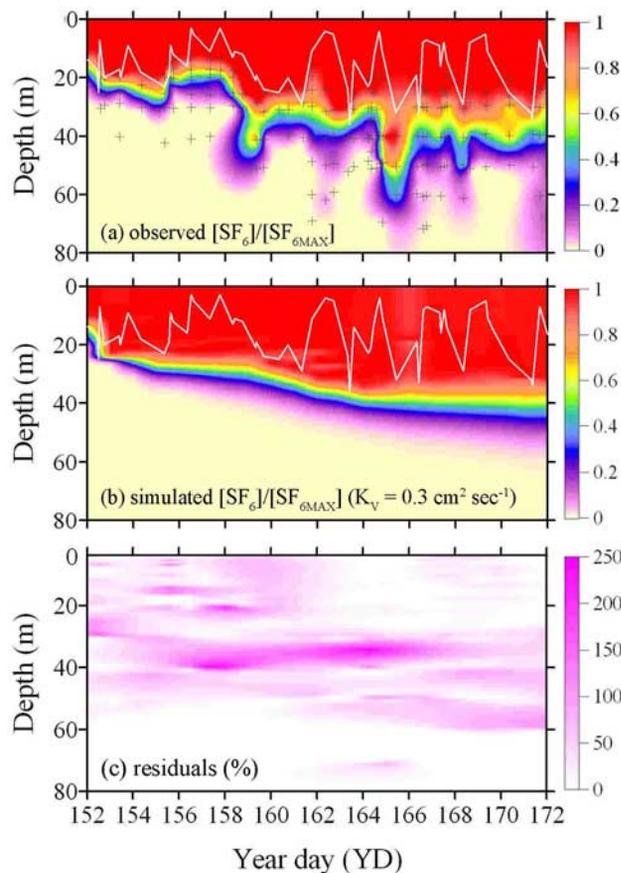
Figure 7. Contour plots of the time evolution of (a) measured and (b) modeled profiles of $[SF_6]$ normalized to the maximum concentration ($[SF_{6MAX}]$) near the base of the mixed layer. The solid line represents measured mixed layer depths (m) and the plus symbols represent sampling depths. (c) Residual plots of ΔSF_6 where ΔSF_6 (%) = $\{(\text{measured } [SF_6] - \text{modeled } [SF_6])/\text{measured } [SF_6]\} \times 100$.

possibility is that the local $[SF_6]/[SF_{6MAX}]$ maximums were caused by advective transport of SF_6 through deepening of the surface mixed layer rather than by diapycnal diffusive transport of SF_6. If this proposed hypothesis had been correct, the local $[SF_6]/[SF_{6MAX}]$ maximums should have persisted during the periods following YD 159.4 or 165.4. The local $[SF_6]/[SF_{6MAX}]$ maximums disappeared in $[SF_6]$ profiles obtained after YD 159.4 or 165.4. Therefore the proposed hypothesis is not a probable mechanism for the formation of the subsurface $[SF_6]/[SF_{6MAX}]$ maximums in the two $[SF_6]/[SF_{6MAX}]$ profiles obtained at YD 159.4 and 165.4.

[20] During the present GasEx-98 experiment, a diurnal study of nutrient dynamics was also performed. The nitrate concentration in the surface mixed layer was found to increase by $\sim$80 nM during the night [*Zhang et al.*, 2001]. If a K_V of 1.0 cm^2 s^{-1} is used, this increase in nitrate concentration in the surface mixed layer during the night could be entirely accounted for by an upward diffusive flux of nitrate. However, the cooling of the surface water during the night would likely cause entrainment of nitrate in deep water to the surface by convective mixing. If the value of K_V = 0.3 cm^2 s^{-1} obtained in the present study is used, the estimate of new production based on the nitrate inven-

tory change in the mixed layer should be scaled down by 30%.

3.6. Sources of Uncertainties in Estimated K_V

[21] Several factors could give rise to uncertainty in the estimation of K_V using the vertical penetration of SF_6 into the upper thermocline. One factor that may cause a significant error in the modeling of K_V is the isopycnal transport of SF_6 in the upper thermocline. To accurately model K_V (see Figure 5), the effect of the isopycnal diffusion process on the evolution of SF_6 concentration for each layer in the upper thermocline should be taken into account, which in turn affects the evolution of the vertical gradient of SF_6 concentration ($d[SF_6]/dZ$) in the upper thermocline. The estimation of the error in the modeled K_V due to the lateral dispersion of SF_6 is discussed in detail in the subsequent section.

[22] Another factor is variation in the distance between the daily occupied hydrographic stations and the corresponding patch center. The further a hydrographic cast is from the patch center, the shorter the period of time for downward penetration of SF_6. In this analysis, the patch center was chosen as the location at which the daily maximum $[SF_6]$ was found. This assumes that the center was found during each daily survey. In the present work, some of the $[SF_6]$ profiles were obtained from hydrographic casts away from the patch center; this effect could cause an error in the estimation of K_V. To assess the effect of station locations relative to the patch center, we constrained the model by $[SF_6]$ profiles whose surface concentrations are higher than 50% of the daily maximum $[SF_6]$ (n = 24). Using this constraint, we obtained a K_V value of 0.35 cm^2 s^{-1}, which is not statistically different from the value of K_V (0.3 cm^2 s^{-1}) obtained using all the $[SF_6]$ profiles.

[23] Temporal variability in the SF_6 background can also be a potential source of errors in the estimation of K_V; however, the effect of such variations appears to be negligible because, over the 3 week period of the experiment, the background for SF_6-uncontaminated waters remained almost constant (0.6–1.0 fM) and is small compared to SF_{6MAX} (2000–4000 fM).

3.7. Evaluation of Errors

[24] Estimating K_V from the 3 week evolution of the $[SF_6]/[SF_{6MAX}]$ profile can be inaccurate if lateral dispersion of SF_6 is ignored or inaccurately represented in the model. Therefore the overall uncertainty in the K_V value was estimated by assuming that uncertainty in modeling the lateral dispersion of SF_6 is the dominant source of error. To quantify the effect of uncertainty in the lateral dispersion of SF_6 on the estimation of K_V, we analyzed the model under three different cases. First, we performed the calculations for conditions where there is no lateral dispersion of SF_6. When we constrained the model with $[SF_6]$ profiles without the lateral dispersion of SF_6, we obtained a K_V of 0.1 cm^2 s^{-1} (Figure 8b), which is smaller than the value (K_V = 0.3 cm^2 s^{-1}) obtained using the measured rate of lateral dispersion (Figures 7b and 8a). In the absence of lateral dispersion, the maximum $[SF_6]$ appeared to migrate into the upper thermocline as the experiment proceeded. This vertical migration of the maximum $[SF_6]$ is not seen in the field data and in the other modeled results. Another feature found
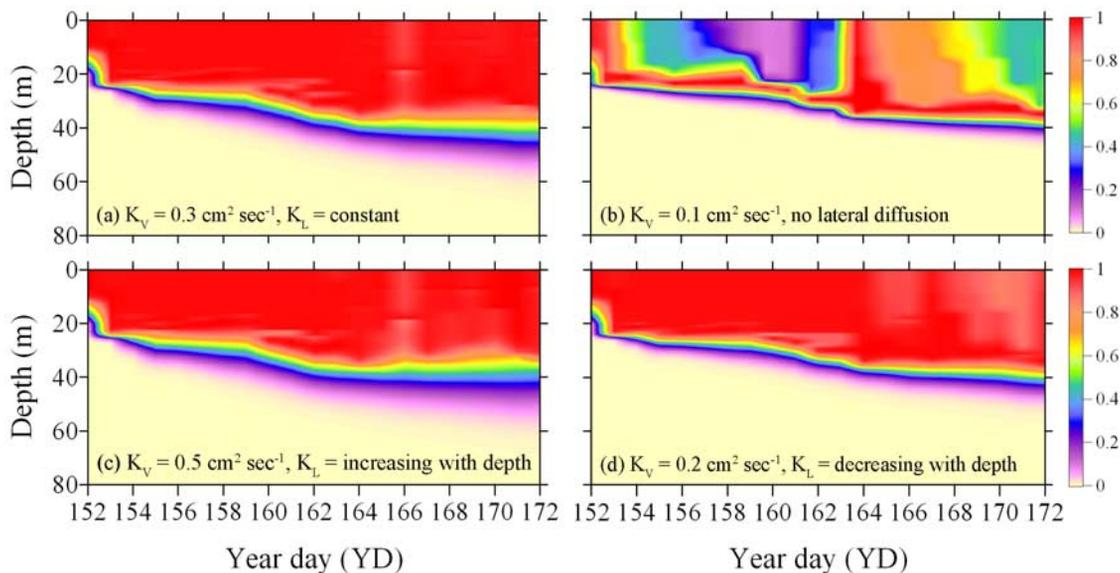
Figure 8. Comparison of the time evolution of modeled profiles of $[SF_6]/[SF_{6MAX}]$ for (a) a measured constant rate of lateral dispersion of SF_6, (b) no lateral dispersion of SF_6, (c) an increasing rate of lateral dispersion of SF_6 with depth, and (d) a decreasing rate of lateral dispersion of SF_6 with depth. K_L denotes the lateral dispersion rate. In Figures 8c and 8d the measured constant rate of lateral diffusion of SF_6 was increased or decreased by 15% with depth in the 20–60 m depth range.

in this scenario is a wide range of $[SF_6]/[SF_{6MAX}]$ in the surface mixed layer. The rate of $[SF_6]$ decrease in the uppermost thermocline (solely due to diapycnal diffusion) was several orders of magnitude lower than that observed in the surface mixed layer (largely due to lateral diffusion and the loss to the atmosphere). Such differential decrease in $[SF_6]$ led to a wide range of $[SF_6]/[SF_{6MAX}]$ in the surface mixed layer. In the second scenario, the lateral dispersion rate of SF_6 was increased with depth (or density) over the 20–60 m depth range. The model using the increasing rate of lateral dispersion yielded a diapycnal diffusivity of $K_V = 0.5$ cm^2 s^{-1} (Figure 8c), which is greater than the value modeled with the constant rate of lateral dispersion. However, higher values of the $[SF_6]/[SF_{6MAX}]$ contour line (e.g., 0.8 = 80% of the maximum $[SF_6]$) tended to be found closer to the surface. Such a trend was not found in the field data. In the third scenario, the lateral dispersion was decreased with depth (or density) over the depth range of 20–60 m. If the model used the decreasing rate of lateral dispersion, it would yield a K_V value of 0.2 cm^2 s^{-1} (Figure 8d). In the second and third scenarios, the measured rate of lateral diffusion of SF_6 was increased or decreased by 15% with depth in the 20–60 m depth range. The evolution of modeled SF_6 profile for the three cases is also not consistent with the measured profile.

[25] The overall difference between the measured dispersion rate-based K_V and the values based on the three cases is ± 0.2 cm^2 s^{-1}. We believe that this is a reasonable approximation to the magnitude of the uncertainty in the estimated K_V value.

3.8. Comparison With Other SF_6-Based Determinations of K_V

[26] Field experiments using SF_6 to measure K_V have been conducted in the permanent thermocline/deep waters [e.g., *Ledwell and Watson*, 1991; *Ledwell and Bratkovich*, 1995; *Ledwell et al.*, 1998] or in waters immediately below the surface mixed layer [*Law et al.*, 1998, 2001, 2003]. The duration of experiments (6–30 months) conducted in the permanent thermocline and deep waters is considerably longer than that of the experiments (days to weeks) performed in waters below the surface mixed layer. Measured values of K_V for the permanent thermocline and deep oceans decrease with increasing water column stratification (N) from basin to basin, as proposed for the ocean by *Gargett* [1984]. One exception to this generalization is the boundary regions of the oceans where diapycnal mixing is several times greater than the value observed in the interior [*Ledwell and Bratkovich*, 1995; *Ledwell et al.*, 2000]. The measured values of K_V for waters below the mixed layer varied considerably from ~ 0.2 cm^2 s^{-1} for the IRONEX-I and SOIREE studies to 2 cm^2 s^{-1} for the PRIME study (Table 1). Our K_V value of 0.3 cm^2 s^{-1} is close to the values estimated from the IRONEX–I and SOIREE data. The large differences between these values determined from the IRONEX–I, SOIREE, and our data and the value from the PRIME data may reflect geographic variations in K_V that exist in the upper thermocline immediately below the mixed layer.

[27] Attempts have been made in relating K_V to water column stratification, internal wave activity, and roughness of the neighboring ocean topography. The general consensus has been that the stratification is an important parameter affecting diapycnal mixing, particularly when the source of energy is from the breaking of the internal wave field [*Gargett*, 1984]. However, presently available values of SF_6-based K_V, averaged over the longer period (weeks to months), support the more recent findings that the diapycnal diffusion rate in the stratified ocean is independent of the water column stratification [*Gregg*, 1989; *Toole et al.*, 1994; *Polzin et al.*, 1995; *Kunze and Sanford*, 1996; *Gregg et al.*, 2003]. The fact that the turbulence responsible for diapycnal

Table 1. Summary of K_V Estimated From Independent Studies Measuring the Vertical Spreading of SF_6 Injected in the Permanent Thermocline or Immediately Below the Base of the Surface Mixed Layer

Location	Depth Range, m	Duration, days	N, cph	K_V, cm^2 s^{-1}
Permanent Thermocline				
Santa Monica Basin	790 ± 100	171	1.1	0.25 ± 0.08
Santa Cruz Basin	1500 ± 400	540	0.2	1.0 ± 0.4
NATRE[a]	300 ± 200	900	2.6	0.17 ± 0.02
Below Surface Mixed Layer				
IRONEX-I[b]	<100	4	7.3	0.25 ± 0.07
PRIME[c]	<100	9	4.4	2.93 ± 0.27
SOIREE[d]	<100	13	5.7	0.11 ± 0.2
GasEx-98 (present study)	<100	21	8.2	0.3 ± 0.2

[a]NATRE is the North Atlantic Tracer Release Experiment, which took place in the southeastern part of the subtropical gyre from early 1992 to late1994 [*Ledwell et al.*, 1998].

[b]IRONEX-I is the Iron Enrichment Experiment conducted in the equatorial Pacific Ocean in 1995 [*Law et al.*, 1998].

[c]PRIME is the U.K. Plankton Reactivity in the Marine Environment program conducted in an anticyclonic eddy at 60°N in the North Atlantic Ocean [*Law et al.*, 2001].

[d]SOIREE is the Southern Ocean Iron Enrichment Experiment conducted at 61°S and 140°E [*Law et al.*, 2003].

mixing is extremely intermittent in time and space makes it difficult to characterize diapycnal diffusion-induced mixing processes [*Gregg et al.*, 2003]. Furthermore, the observations needed to measure such a parameter are technically demanding. Nonetheless, many more SF_6-based experiments and careful analysis of resulting data will be needed to clarify diapycnal diffusive mixing processes. Such understanding should lead to parameterizations that can be used to represent diapycnal diffusive mixing in the oceans.

4. Conclusion and Future Study

[28] In the present study, we determined apparent diapycnal diffusivity, K_V, of 0.3 ± 0.2 cm^2 s^{-1} using the 1-D Fickian diffusion model constrained with data for the evolution of the $[SF_6]$ profiles that were collected in the eastern North Atlantic Ocean during the GasEx-98 cruise. The estimated K_V represents an average over a 3 week period for a layer of depth of 20–60 m in an anticyclonic eddy. The use of the Fickian model, including a lateral diffusion component, facilitates reproduction of the time evolution of $[SF_6]$ for each isopycnal surface. The accurate representation of the time evolution of $[SF_6]$ for each isopycnal surface is important in the accurate estimation of K_V.

[29] A more robust way to measure K_V near the surface mixed layer is to release SF_6 at a specific density surface below the base of the surface mixed layer and then to measure the diapycnal spreading of SF_6 with time. This type of tracer experiment needs to be performed in different oceanic regions and in different seasons to determine key factors controlling the vertical transport of SF_6 in the upper thermocline wherein upward fluxes of nutrients into the mixed layer constrain on net primary productivity.

References

Bryan, F. (1987), Parameter sensitivity of primitive equation ocean general circulation models, *J. Phys. Oceanogr.*, *17*, 970–985.

Eppley, R. W., and B. J. Peterson (1979), Particulate organic matter flux and planktonic new production in the deep ocean, *Nature*, *282*, 677–680.

Ewart, T. E., and W. P. Bendiner (1981), An observation of the horizontal and vertical diffusion of a passive tracer in the deep ocean, *J. Geophys. Res.*, *86*, 10,974–10,982.

Gargett, A. E. (1984), Vertical eddy diffusivity in the ocean interior, *J. Mar. Res.*, *42*, 359–393.

Gargett, C. (1993), A stirring tale of mixing, *Nature*, *364*, 670–671.

Gregg, M. C. (1989), Scaling turbulent dissipation in the thermocline, *J. Geophys. Res.*, *94*, 9689–9698.

Gregg, M. C., T. B. Sanford, and D. P. Winkel (2003), Reduced mixing from the breaking of internal waves in equatorial waters, *Nature*, *422*, 513–515.

Kunze, E., and T. B. Sanford (1996), Abyssal mixing: Where it is not, *J. Phys. Oceanogr.*, *26*, 2286–2296.

Law, C. S., A. J. Watson, M. I. Liddicoat, and T. Stanton (1998), Sulphur hexafluoride as a tracer of biogeochemical and physical processes in an open-ocean iron fertilization experiment, *Deep Sea Res., Part II*, *45*, 977–994.

Law, C. S., A. P. Martin, M. I. Liddicoat, A. J. Watson, K. J. Richards, and E. M. S. Woodward (2001), A Lagrangian SF_6 tracer study of an anticyclonic eddy in the North Atlantic: Patch evolution, vertical mixing and nutrient supply to the mixed layer, *Deep Sea Res., Part II*, *48*, 705–724.

Law, C. S., E. R. Abraham, A. J. Watson, and M. I. Liddicoat (2003), Vertical eddy diffusion and nutrient supply to the surface mixed layer of the Antarctic Circumpolar Current, *J. Geophys. Res.*, *108*(C8), 3272, doi:10.1029/2002JC001604.

Ledwell, J. R., and A. Bratkovich (1995), A tracer study of mixing in the Santa Cruz Basin, *J. Geophys. Res.*, *100*, 20,681–20,704.

Ledwell, J. R., and A. J. Watson (1991), The Santa Monica Basin tracer experiment: A study of diapycnal and isopycnal mixing, *J. Geophys. Res.*, *96*, 8695–8718.

Ledwell, J. R., A. J. Watson, and C. S. Law (1998), Mixing of a tracer in the pycnocline, *J. Geophys. Res.*, *103*, 21,499–21,529.

Ledwell, J. R., E. T. Montgomery, K. L. Polzin, L. C. St. Laurent, R. W. Schmitt, and J. M. Toole (2000), Evidence for enhanced mixing over rough topography in the abyssal ocean, *Nature*, *403*, 179–182.

Lewis, M. R., W. G. Harrison, N. S. Oakey, D. Herbert, and T. Platt (1986), Vertical nitrate fluxes in the oligotrophic ocean, *Science*, *234*, 870–872.

McGillis, W. R., J. B. Edson, J. E. Hare, and C. W. Fairall (2001), Direct covariance air-sea CO_2 fluxes, *J. Geophys Res.*, *106*, 16,729–16,745.

Merlivat, L., and P. Brault (1995), CARIOCA buoy: Carbon dioxide monitor, *Sea Technol.*, *36*, 23–30.

Munk, W. H. (1966), Abyssal recipes, *Deep Sea Res*, *13*, 707–730.

Park, G.-H., K. Lee, C.-M. Koo, H.-W. Lee, C.-K. Lee, J.-S. Koo, T. Lee, S.-H. Ahn, H.-G. Kim, and B. K. Park (2005), A sulfur hexafluoride-based Lagrangian study on initiation and accumulation of the red tide *Cochlodinium polykrikoides* in southern coastal waters of Korea, *Limnol. Oceanogr.*, *50*, 578–586.

Polzin, K. L., J. M. Toole, and R. W. Schmitt (1995), Fine-scale parameterizations of turbulent dissipation, *J. Phys. Oceanogr.*, *25*, 306–328.

Price, J. F., R. A. Weller, and R. Pinkel (1986), Diurnal cycling: Observations and models of the upper ocean response to diurnal heating, cooling, and wind mixing, *J. Geophys. Res.*, *91*, 8411–8427.

Schuert, E. A. (1970), Turbulent diffusion in the intermediate waters of the North Pacific Ocean, *J. Geophys. Res.*, *75*, 673–682.

Toole, J. M., K. L. Polzin, and R. W. Schmitt (1994), Estimates of diapycnal mixing in the abyssal ocean, *Science*, *264*, 1120–1123.

Upstill-Goddard, R. C., A. J. Watson, M. I. Liddicoat, and J. Wood (1991), Sulphur hexafluoride and Helium-3 as seawater tracers: Deployment techniques and continuous underway analysis of SF_6 and cryotrap EC-GC, *Anal. Chem.*, *249*, 555–562.

Vasholz, D. P., and L. J. Crawford (1985), Dye dispersion in the seasonal thermocline, *J. Phys. Oceanogr.*, *15*, 695–712.

Wanninkhof, R., and W. R. McGillis (1999), A cubic relationship between air-sea CO_2 exchange and wind speed, *Geophys. Res. Lett.*, *26*, 1889–1892.

Wanninkhof, R., et al. (1997), Gas exchange, dispersion, and biological productivity on the west Florida shelf: Results from a Lagrangian tracer study, *Geophys. Res. Lett.*, *24*, 1767–1770.

Watson, A. J., R. C. Upstill-Goddard, and P. S. Liss (1991), Air-sea gas exchange in rough and stormy seas measured by a dual tracer technique, *Nature*, *349*, 145–147.

Woods, J. D. (1968), Wave-induced shear instability in the summer thermocline, *J. Fluid Mech.*, *32*, 791–800.

Zhang, J. Z., R. Wanninkhof, and K. Lee (2001), Enhanced new production observed from the diurnal cycle of nitrate in an oligotrophic anticyclonic eddy, *Geophys. Res. Lett.*, *28*, 1579–1582.

———————————

Y.-S. Chang, S.-D. Choi, D.-O. Kim, and K. Lee (corresponding author), School of Environmental Science and Engineering, Pohang University of Science and Technology, San 31, Hyoja-dong, Nam-gu, Pohang, 790-784, Korea. (yschang@postech.ac.kr; skills@postech.ac.kr; nandama@postech.ac.kr; ktl@postech.ac.kr)

H.-S. Kang and J.-Z. Zhang, Atlantic Oceanographic and Meteorological Laboratory/NOAA, 4301 Rickenbacker Causeway, Miami, FL 33149, USA. (heesook.kang@noaa.gov; jia-zhong.zhang@noaa.gov)